J Mater Sci: Mater Med (2007) 18:2011–2015
DOI 10.1007/s10856-007-3102-x

Surface characterization of colloidal-sol gel derived biphasic HA/FA coatings

Kui Cheng · Sam Zhang · Wenjian Weng

Received: 6 March 2006 / Accepted: 14 June 2006 / Published online: 9 June 2007

Abstract Hydroxyapatite (HA) powders are ultrasonically dispersed in the precursor of fluoridated hydroxyapatite (FHA) or fluorapatite (FA) to form a ''colloidal sol''. HA/FA biphasic coatings are prepared on Ti6Al4V substrate via dip coating, 150 °C drying and 600 °C firing. The coatings show homogenous distribution of HA particles in the FA matrix. The relative phase proportion can be tailored by the amount of HA in the colloidal sol. The surfaces of the coatings consist of two kinds of distinct domains: HA and FA, resulting in a compositionally heterogeneous surface. The biphasic coating surface becomes increasingly rougher with HA powders, from around 200 nm of pure FA to 400–600 nm in Ra of biphasic coatings. The rougher biphasic HA/FA surfaces with chemically controllable domains will favor cell attachment, apatite layer deposition and necessary dissolution in clinical applications.

Introduction

Hydroxyapatite (HA) coated metallic implants have been widely investigated due to their fast integration with bone comparing with pure metal [1, 2]. In order to improve their holistic performance in vivo, researches have focused on the following respects: (i) Inducing active interaction between the coating and tissue through promotion of osteoblast cell attachment, proliferation and differentiation, resulting in fast new bone formation and osteointegration [3, 4]; (ii) Making coatings more dissolution-resistant through reduction of intrinsic solubility of the coating materials, so that better long-term effectiveness of the implants could be obtained [5, 6].

Fluorine substitution in HA structure results in fluoridated hydroxyapatite (FHA), a solid solution between HA and fluorapatite (FA) [7]. FHA coatings have the ability to modify physicochemical properties and thus are able to meet the above-mentioned long term stability target [8–11]. However, from cell proliferation point of view, pure HA is preferred because large dissolution of HA leads to increases of Ca and P ion concentrations that favor cell activities [12, 13]. Although long term stability (dissolution resistance) and enhanced cell attachment are achieved on FHA coatings, cell proliferation is compromised because release of Ca and P ions is impaired [14]. To strike a balance between these two polarities, FHA coatings with moderate F content are tested and they do demonstrate good performances both in vitro and in vivo [14, 15].

Based on these findings, conceptually, a ''two-in-one'' HA/FA biphasic coating could provide an even better alternative: while the FA phase provides a favorable surface for cell attachment and the HA phase provides necessary dissolution to favor cell activities. In realization of this ''two-in-one'' concept, the structure of the coating must be carefully controlled: (1) both FA and HA phases are exposed to provide a platform for cell attachment and ion release; (2) the HA phase only exists in the surface layer of the coatings, i.e., a pure FA bottom layer should exist between the surface layer and the substrate to ensure

K. Cheng · S. Zhang (✉)
School of Mechanical and Aerospace Engineering,
Nanyang Technological University, 50 Nanyang Avenue,
Singapore 639798, Singapore
e-mail: msyzhang@ntu.edu.sg

W. Weng
Department of Materials Science and Engineering,
Zhejiang University, Hangzhou 310027, P.R. China

the long-term dissolution resistance. Since the bottom FA layer could be easily prepared based on previous work [14], the distribution of HA in FA matrix is of special interest. Moreover, whether the existence of HA particles in the coating will affect the roughness or not is also important, since it has reported rough surface are favorable for cell attachment [16, 17].

In our recent work [18], an effective colloidal-sol gel method was developed to prepare biphasic calcium phosphate coatings. In this work, HA/FA biphasic coatings are prepared in a similar way, and we look into the surface characteristics and HA distribution of these coatings.

Materials and methods

Calcium nitrate tetrahydrate ($Ca(NO_3)_2{\cdot}4H_2O$, GR, Merck) and phosphor pentoxide (P_2O_5, GR, Merck) were dissolved in ethanol (GR, Merck) respectively to form the 2mol/L ''Ca-solution'' and ''P-solution''. After the ''P-solution'' was refluxed for 24 h, designed amount of hexafluorophosphoric acid (HPF_6, GR, Merck) was added drop-wise in a rate of 5mL/min. Then, the ''Ca-solution'' was added to form the FHA precursors with Ca:P:F ratio of 5:3:1 and 15:9:2. Commercial HA powders (GR, Merck) were added into the FHA precursor in $Ca_{powder}/Ca_{precursor}$ ratio of 1/4, 1/2, 3/4 and 1/1. After 20 min ultrasonic dispersing, the colloidal sols were obtained.

Titanium alloy (Ti-6Al-4V) substrates were polished down to #1200 grade SiC paper. The substrates were rinsed in double distilled water and ultrasonically washed in acetone for ten minutes and dried before coating. The substrates were dipped in the colloidal sols and withdrawn at a speed of 15 cm/min. After 15 min drying in oven at 150 °C and 15 min firing at 600 °C, a single layer of the coatings was obtained. Such dipping and heat treatment process were repeated once to increase the thickness of the coating. As a comparison, FHA and FA coatings were also prepared using the precursors with Ca:P:F ratio of 15:9:2 and 5:3:1 respectively.

X-ray Diffractometry (XRD, RIGAKU, D-Max, RA, with a 2°/min scanning speed and step of 0.02°, scanning range from 20° to 40°) was used to characterize the crystalline phase of the coatings. The chemical composition of the surface was characterized through X-ray Photoelectron Spectroscopy (XPS, AXIS Kratos Ultra, Aluminum mono, 1 eV per step for survey scan, 0.1 eV per step for narrow scan), and Fourier Transformed Infrared Spectroscopy (FTIR, Bio-rad, with 2 cm^{-1} resolution). The surface morphology of the coatings was observed with the Scanning Electron Microscopy (SEM, JEOL, JSM5600LV) after a gold layer was sputtered on coatings' surface. The roughness of the coating was characterized in an optical profiler imaging system (WYKO, NT2000, Veecco Instruments Inc, USA), a 736 μm × 480 μm area was analyzed. The coating sample was embedded in resin and polished from cross-sectional direction down to #2000 grade SiC paper, then observed at SEM for the thickness. Typically, the thickness of the coatings was around 1–4 μm [18].

Results

Figure 1 provides evidence that all the coatings obtained are of apatite phase where diffraction peaks belonging to (211), (112), (300), (002) and (202) are clearly seen. In FHA coatings, these peaks are located at rather high diffraction angles, (JCPDS 15–876). These peaks are significantly widened in the coatings derived from the colloidal sols. The FWHM (Full Width at Half Maximum) of the (300) peaks are tabulated in Table 1 for easy comparison. The FHA coatings obtained from as-refluxed sols have obvious smaller FWHM (0.278° for FHA and 0.279° for FA) than those from the colloidal sols (0.365°, 0.579°, 0.389° and 0.603° for the other coatings respectively).

Figure 2 is typical XPS survey scan results of both the conventional FHA coating and the biphasic coating. It is quite clear that all the surfaces contain Ca, P, O and F. The exact F contents of the coatings in term of F/Ca ratios are also tabulated in Table 1: the F/Ca ratio of the FHA coating is 0.148. In pure FA, the F/Ca ratio is 2.00. In the biphasic coatings, the F/Ca ratio decreases with increasing $Ca_{powder}/Ca_{precursor}$ ratio, or: 0.171, 0.168, 0.152 and 0.140.

Figure 3 shows surface morphologies of the coatings: the FHA and FA coatings are smooth and homogeneous (Figure 3a) but the biphasic coatings become rougher (Figure 3b, c) with increasing amount of HA powders in the colloidal sols. On the biphasic coating surface, more particles are observed with increasing degree of HA pow-

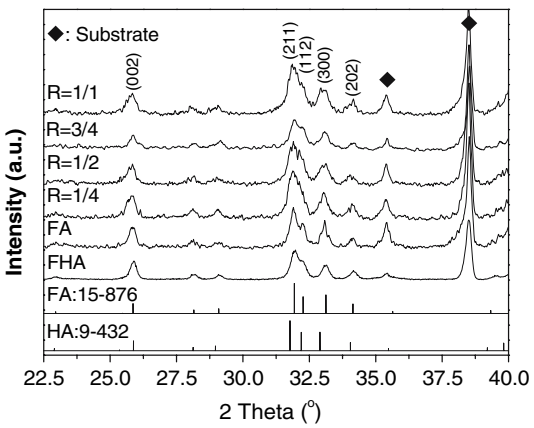

Fig. 1 XRD patterns of the coatings (R: $Ca_{powder}/Ca_{precursor}$)

Table 1 The FWHM of (300) peak as well as the F content of the coatings (R: $Ca_{powder}/Ca_{precursor}$)

Sample Annotation	FHA	FA	R = 1/4	R = 1/2	R = 3/4	R = 1/1
FWHM of (300) peak (°)	0.278	0.279	0.365	0.579	0.389	0.605
F/Ca ratio (mol/mol)	0.148	0.200	0.171	0.168	0.152	0.140

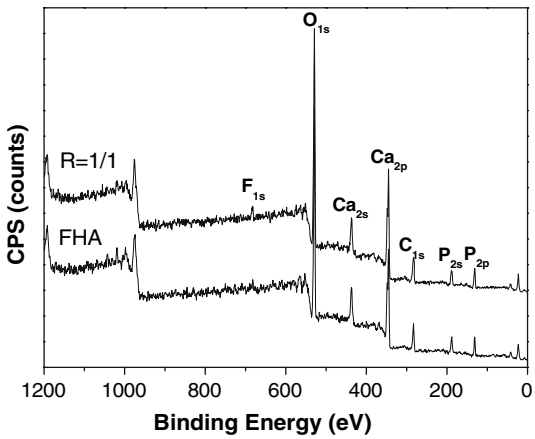

Fig. 2 Typical XPS spectra of the conventional FHA coating and the colloidal-sol derived biphasic coating of R = 1 (R: $Ca_{powder}/Ca_{precursor}$)

der incorporation. Meanwhile, the surface crack density becomes increasingly higher as well.

Discussion

The crystalline phase of the coatings

The HA and FA coatings obtained have almost the same XRD patterns due to their similar crystallographic structures, except for minor differences in lattice parameters, especially a, (HA: a = 0.942 nm, JCPDS 9–432, FA: a = 0.937 nm, JCPDS 15–876). As solid solutions between HA and FA, FHA has a lattice parameter between HA and FA. As a result, the diffraction peaks (especially those lattices perpendicular to c axis) of FHA and FA will locate at relative higher angle depending on the F content. In Figure 1, in contrast to the standard pattern of HA, the diffraction peaks of FHA coatings shift to higher angles with increasing F, indicating a good correlation between the F content and lattice parameter of the coating [19].

If the coatings are biphasic, the structure of both phases are not changed, thus there should be no change in lattice parameters. Since the XRD spot size is too big to distinguish the phases, the pattern is a mixture of the two, showing as significantly widened peaks. In Table 1, the width of (300) peaks are compared, those colloidal-sol coatings show significantly larger values: 0.365°, 0.579°, 0.389° and 0.603°, comparing with 0.278 and 0.279 of FHA coatings. Therefore, the widening of the (300) peaks actually demonstrates the HA particle was not fluoridated during the preparation, HA/FA biphasic coatings have been obtained as expected.

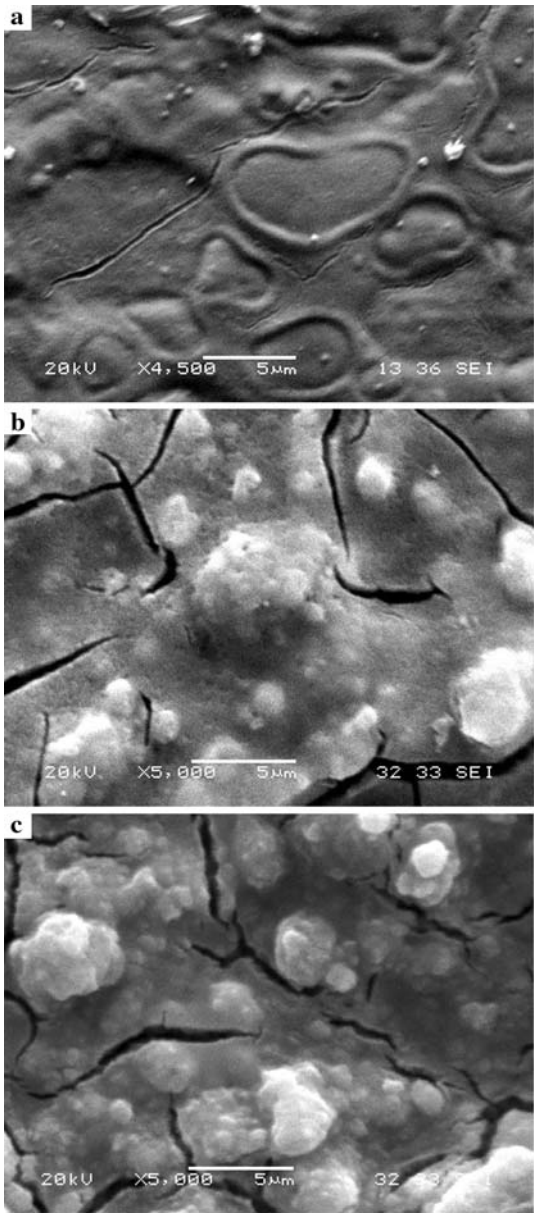

Fig. 3 SEM micrographs of (**a**) conventional FHA coating and the colloidal-sol derived biphasic coatings of (**b**) R = 1/2 and (**c**) R = 1/1 (R: $Ca_{powder}/Ca_{precursor}$)

The surface chemical composition

As HA is expected to provide rather dissolved Ca^{2+} and PO_4^{3-} during the early stage of implantation in real cases, it is of special interest to know if they are exposed on the very surface of the coating. In Figure 2, the XPS results show all the FHA coatings and HA/FA coatings show the existence of Ca, P, O and F. However, due to the similar structure of FA, FHA and HA, their chemical environments of the elements are quite similar, the binding energy of the elements only shift a little [20], which makes it difficult to distinguish FHA and HA/FA coatings through peak deconvolution.

However, the F content obtained by XPS in term of F/Ca ratios could give some clue on the relative phase content. That is because the XPS results actually collects signal from only about 10 nm deep in the surface of selected areas (in this work, the effective area is around 300 μm × 700 μm). The F/Ca ratio was obtained by comparing the total counts of F and Ca throughout the effective area. For the biphasic coatings, since all of their FHA precursors have the same HPF_6 content, the F/Ca ratio variations actually result from HA content variations. Therefore, in Table 1, the decreasing F content of the coating actually means the increases of HA amount.

The reflection spectra of FTIR in Figure 4 give more information on surface chemical groups: all the FHA coatings and HA/FA coatings show the existence of PO_4^{3-}, OH^- and CO_3^{2-}. Among them, the OH stretching band show significant difference: a very weak bands located at 3537cm^{-1} is observed on FHA coatings, which is reported to be from the sporadic OH groups in the F chain [21]; no such band is observed on FA coating. While for the biphasic coatings, the intensity of this band becomes increasingly higher with increasing amount of HA in the coating. These results prove that the amount of OH groups on coating surface is proportional to the HA amount in the coatings, i.e., more HA powders expose on the surface.

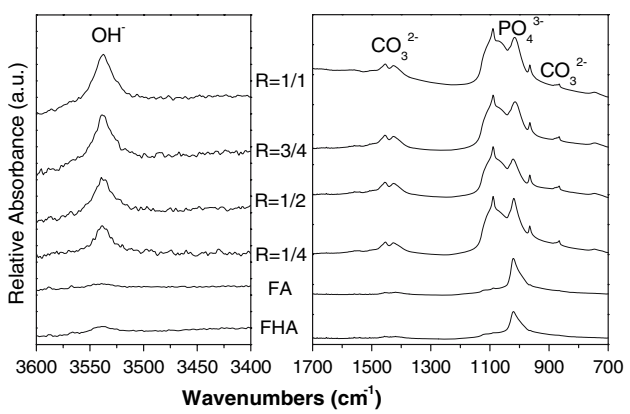

Fig. 4 FTIR spectra of the biphasic coatings (R: $Ca_{powder}/Ca_{precursor}$)

It is noteworthy that the position of these stretching bands is different from that in pure HA (3573cm^{-1}, [21]). This happens in FHA, too (3537cm^{-1}, [21]). Since such shift is the effect of hydrogen bonding between F and OH [22, 23], the difference could be possibly come from minor F adsorption on the powder or hydrogen bonding between OH in the HA powders and F in the peripheral FA matrix.

Both XPS and FTIR reflection spectra demonstrate that the existence of HA powders renders the HA/FA biphasic coatings unique surface characteristics in contrast to FHA: although the F content could be similar, the chemical groups on the surface are quite different, FHA coating provides homogeneous surface with evenly distributed F, while the biphasic coating shows heterogeneous surface consist of distinguished FA domains and HA regions, with majority of the F existing in the FA domains. Such surface structure could be an optimized one for F containing coatings from composition point of view: The FA domain can act as cell attachment platform with long-term stability, while the HA domain could provide necessary Ca^{2+} and PO_4^{3-} ions releasing, thus the characteristic of both materials are better utilized.

The surface morphology and roughness

As observed in the SEM micrograph in Figure 3, the conventional FHA coatings and the biphasic HA/FA coatings have different surface morphology. In Figure 5, the roughness of the coatings is further compared. The conventional FHA and FA coatings show similar roughness. In HA/FA coatings, however, the roughness increases due to presence of HA powders, which is reasonable since the HA powders will partially protruded from the coating surface. However, as schematically shown in Figure 6, the effect on roughness is not linear: when the amount of the powders is rather small, the powders tend to exist as separated particle, which gives rise to increase of the rough-

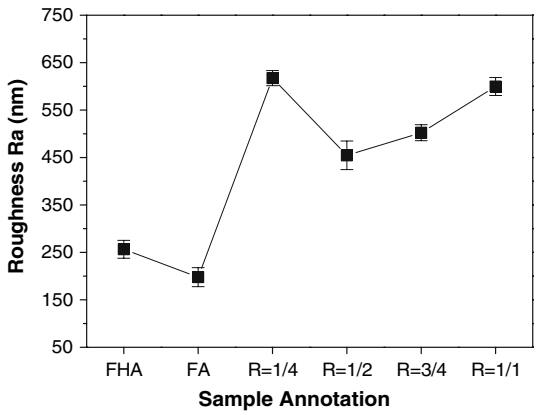

Fig. 5 Surface roughness of the biphasic coatings in comparison with the conventional FHA (R: $Ca_{powder}/Ca_{precursor}$)

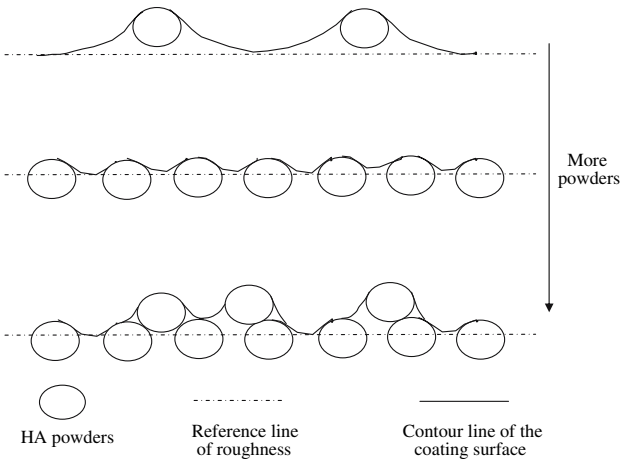

Fig. 6 Schematic figure of the HA powders on coating roughness

ness due to the protrusion of the particles from the reference line in roughness measurement; with the increasing the powders amount, the reference line itself elevated due to the thickening effect of the powders [18], which will result in a slightly decrease of the roughness; with even more powders, the powders began to directly contact each other and even agglomerated, that will lead to even larger protrusion of the powders or agglomerates, which makes the roughness goes up again. Nevertheless, as shown in Figure 5, all these biphasic HA/FA coatings show much higher roughness (Ra = 450–650nm), comparing with FHA coating and FA coating (Ra = 150–200nm).

With the existence and increase of HA phase in the coatings, cracks are observed in the coatings and the number become increasingly large with the increasing amount of powders. That was also attributed to the thickening effect of the particles on coatings [18], which could be further improved by using HA particles with smaller size. Moreover, in the real application, a pure FA layer, which is shown to be dense and crack free in Figure 3a, could be prepared between the HA/FA coating and the substrate, thus prevent the formation of harmful ''through-thickness cracks'', which is harmful to coating-substrate interface. In this situation, these cracks in the top HA/FA top layer, as well as the roughened surface of the coating, could further act as anchorage site for the cells, thus promoting cell attachment.

Conclusion

1. The colloidal-sol-gel route is an effective way in deposition of biphasic HA/FA coatings. The relative phase content in the resulted coating can be tailored through variation of the amount of HA powder dispersed in the sol.
2. The biphasic HA/FA coating has unique surface characteristics in comparison with the mono phase FHA coating: HA and FA exist in distinguished domains leading to heterogeneous coating surface.
3. The existence of HA powders leads to rougher surfaces. Roughness of the surface can be tailored to certain extent by varying the amount of HA powders.

Acknowledgement The author would like to thank the Agency for Science Technology and Research, Singapore (A*Star project 032 101 0005) for the financial support.

References

1. K. De GROOT, R. GEESINK, C. P. A. T. KLEIN and P. SEREKIAN, *J. Biomed. Mater. Res.* **21** (1987) 1375
2. J. L. ONG, D. L. CARNES and K. BESSHO, *Biomaterials.* **25** (2004) 4601
3. K. OGATA, S. IMAZATO, A. EHARA, S. EBISU, Y. KINOMOTO, T. NAKANO and Y. UMAKOSHI, *J. Biomed. Mater. Res.* **72A** (2005) 127
4. M. STEWART, J. F. WELTER and V. M. GOLDBERG, *J. Biomed. Mater. Res.* **69A** (2004) 1
5. L. GINESTE, M. GINESTE, X. RANZ, A. ELLEFTERION, A. GUILHEM, N. ROUQUET and P. FRAYSSINET, *J. Biomed. Mater. Res.* **48** (1999) 224
6. S. OVERGAARD, M. LIND, K. JOSEPHSEN, A. B. MAUNSBACH, C. BOGER and K. SOBALLE, *J. Biomed. Mater. Res.* **39** (1998) 141
7. K. CHENG, G. SHEN, W. WENG, G. HAN, J. M. F. FERREIRA and J. YANG, *Mater. Lett.* **51** (2001) 37
8. H. KIM, Y. KONG and J. C. KNOWLES, *Biomaterials.* **25** (2004) 3351
9. D. FERRO, S. M. BARINOV, J. V. RAU, R. TEGHIL and A. LATINI, *Biomaterials.* **26** (2005) 805
10. K. A. BHADANG and K. A. GROSS, *Biomaterials.* **25** (2005) 4935
11. K. CHENG, W. WENG, H. QU, P. DU, G. SHEN, G. HAN, J. YANG and J. M. F. FERREIRA, *J. Biomed. Mater. Res.* **69B** (2004) 33–37
12. Y. L. CHANG, C. M. STANFORD and J. C. KELLER, *J. Biomed. Mater. Res.* **52** (2000) 270
13. S. MAENO, Y. NIKI, H. MATSUMOTO, H. MORIOKA, T. YATABE, A. FUNAYAMA, Y. TOYAMA, T. TAGUCHI and J. TANAKA, *Biomaterials.* **26** (2005) 4847
14. K. CHENG, W. WENG, H. WANG and S. ZHANG, *Biomaterials.* **26** (2005) 6288
15. L. SAVARINO, M. FINI, G. CIAPETTI, E. CENNI, D. GRANCHI, N. BALDINI, M. GRECO, G. RIZZI, R. GIARDINO and A. GIUNTI, *J. Biomed. Mater. Res.* **66A** (2003) 652
16. D. D. DELIGIANNI, N. D. KATSALA, P. G. KOUTSOUKOS and Y. F. MISSIRLIS, *Biomaterials.* **22**(1) (2001) 87
17. P. J. Ter BRUGGE, J. G. C. WOLKE and J. A. JANSEN, *J. Biomed. Mater. Res.* **60**(1) (2002) 70
18. K. Cheng, S. Zhang and W. Weng, *Thin Solid Films.* **515** (2006) 135
19. K. CHENG, G. HAN, W. WENG, H. QU, P. DU, G. SHEN, J. YANG and J. M. F. FERREIRA, *Mater. Res. Bull.* **38** (2003) 89
20. W. J. LANDIS and J. R. MARTIN, *J. Vac. Sci. Technol.* **A2** (1984) 1108
21. G. PENEL, G. LEROY, C. REY, B. SOMBRET, J. P. HUVENNE and E. BRES, *J. Mater. Sci Mater. Med.* **8** (1997) 271
22. F. Freund and R. M. Knobel, *J. Chem. Soc. Dalton.* (1977) 1136
23. M. SHIRKHANZADEH, *J. Mater. Sci. Mater. Med.* **6** (1995) 90